# Lytic transglycosylases mitigate periplasmic crowding by degrading soluble cell wall turnover products

Anna Weaver[1,2*], Laura Alvarez[3*], Kelly Rosch[1], Asraa Ahmed[1,6] Garrett Wang[1], Jung-Ho Shin[1], Michael VanNieuwenhze[4,5], Felipe Cava[3a], and Tobias Dörr[1,2,6a]

[1] Weill Institute for Cell and Molecular Biology, Cornell University, Ithaca, NY 14853, USA
[2] Department of Microbiology, Cornell University, Ithaca NY 14853, USA
[3] The Laboratory for Molecular Infection Medicine Sweden (MIMS), Department of Molecular Biology, Umeå University, 90187 Umeå, Sweden.
[4] Department of Molecular and Cellular Biochemistry, Indiana University, Bloomington, IN 47405, USA
[5] Department of Chemistry, Indiana University, Bloomington, IN 47405, USA
[6] Cornell Institute of Host-Microbe Interactions and Disease, Cornell University, Ithaca NY 14853, USA

*equal contribution
[a] corresponding authors: tdoerr@cornell.edu, felipe.cava@umu.se

## Abstract

The peptidoglycan cell wall is a predominant defining structure of bacteria, determining cell shape and supporting survival in diverse conditions. As a single, macromolecular sacculus enveloping the bacterial cell during growth and division, peptidoglycan is necessarily a dynamic structure that requires highly regulated synthesis of new material, remodeling, and turnover – or autolysis – of old material. Despite ubiquitous clinical exploitation of peptidoglycan synthesis as an antibiotic target, much remains unknown about how bacteria modulate synthetic and autolytic processes. Here, we couple bacterial genetics in *Vibrio cholerae* with compositional analysis of soluble pools of peptidoglycan turnover products to uncover a critical role for a widely misunderstood class of autolytic enzymes, the lytic transglycosylases (LTGs). We demonstrate that LTG activity is specifically required for vegetative growth. The vast majority of LTGs, however, are dispensable for growth, and defects that are ultimately lethal accumulate due to generally inadequate LTG activity, rather than the absence of specific individual enzymes.

Consistent with this, we found that a heterologously expressed *E. coli* LTG, MltE, is capable of sustaining *V. cholerae* growth in the absence of endogenous LTGs. Lastly, we demonstrate that soluble, uncrosslinked, endopeptidase-dependent peptidoglycan chains accumulate in the WT, and, to a higher degree, in LTG mutants, and that LTG mutants are hypersusceptible to the production of diverse periplasmic polymers. Collectively, our results suggest that a key function of LTGs is to prevent toxic crowding of the periplasm with synthesis-derived PG fragments. Contrary to prevailing models, our data further suggest that this process can be temporally separate from peptidoglycan synthesis.

## Introduction

The bacterial cell wall is a nearly universal feature of the bacterial cell envelope. Made primarily of the strong and elastic polymer peptidoglycan (PG), the cell wall preserves bacterial shape while protecting the cell from its high internal turgor pressure and external environmental challenges[1-5]. PG synthesis begins in the cytoplasm with the generation of lipid II, consisting of the disaccharide [N-acetylmuramic acid (MurNAc)-N-acetylglucosamine (GlcNAc)] that is modified with a pentapeptide side stem and attached to the lipid carrier undecaprenol. Lipid II is flipped across the cytoplasmic membrane where the cell wall is assembled in two reactions: First, lipid II is polymerized into longer glycan strands by glycosyltransferases (GTases) followed by crosslinking of the elongating PG strands via their peptide side stems by transpeptidases (TPases)[3,4,6-8]. Ultimately, the combined result of GTase and TPase activities is a covalently closed mesh-like macromolecular network called the PG sacculus.

54 The strength of the PG sacculus is a double-edged sword. On the one hand, the covalent
55 network provides a mechanical structure strong enough to withstand the high cellular
56 turgor pressure and stresses of a changing environment. On the other hand, it acts as a
57 macromolecular cage that might inhibit cellular expansion and division as well as the
58 insertion of crucial trans-envelope machinery (i.e., flagella and pili).[9-14] Bacteria therefore
59 need to couple new PG synthesis with degradation of bonds within the PG network to
60 simultaneously maintain the integrity of the sacculus while also making space for the
61 insertion of new PG.[11,15,16]
62
63 PG degradation is accomplished by several divergent enzyme classes that are often
64 subsumed under the term "autolysins", i.e., enzymes that cleave various bonds within PG.
65 Endopeptidases (EPs), for example, cleave the peptide crosslinks and are particularly
66 integral to the "space-making" autolytic function that permits sacculus expansion during
67 cell elongation; without EP activity, PG synthesis results in a thicker cell wall or integrity
68 failure and lysis.[17,18] Another major class of autolysins, the lytic transglycosylases (LTGs),
69 cleave the glycosidic linkages between disaccharide subunits within PG strands. Their
70 biochemistry has been exquisitely well-studied and the diversity of their structures and
71 mechanisms of action well characterized.[19-22] Unlike the other autolysins, the primary
72 cleavage mechanism of LTGs is non-hydrolytic. Rather, LTGs perform an intramolecular
73 cyclization of MurNac residues to generate a unique and readily identifiable signature of
74 their activity, anhydro-MurNAc (anhMurNAc).[20,23,24] Early characterization of PG in the
75 bacterial sacculus suggested that every PG strand in the sacculus terminates in an
76 anhMurNAc cap, long implicating LTGs as potential "terminases" of GTase glycan

elongation.[23,25] This was only recently confirmed empirically with the novel discovery and characterization of MltG and its functional analogs [26-29]. MltG associates with active PG synthetic complexes to release new strands from the cytoplasmic membrane (to which they are initially tethered via undecaprenyl pyrophosphate), presumably as they emerge from GTase activity; consequently, MltG is a strong determinant of PG strand length.[26-29] Other physiological roles assigned to LTGs include local PG editing for insertion of PG-spanning protein complexes[10,12,30] and PG recycling. PG recycling, the re-incorporation of PG breakdown products into the biosynthesis cycle, starts with re-uptake of PG turnover products by the importer AmpG.[31] AmpG specifically imports LTG breakdown products (anhMurNAc-containing fragments) and this process can theoretically be supported by any active LTG that produces monomeric anhydromuropeptides. Despite being well-conserved throughout many bacterial phyla, PG recycling is not an essential process under standard growth conditions.[32] Another underappreciated function of LTGs has emerged through the work of our group and others wherein certain individual or combinatorial LTG mutations, including septal LTG RlpA, results in a daughter cell separation defect[33-36]

Answering the most general physiological questions about LTGs has been severely encumbered by their redundancy. Many organisms encode several LTGs with presumably overlapping functions and rarely does a single LTG mutation yield a significant, readily investigable phenotype. The genetic and functional redundancy displayed by LTGs is consistent with an important conserved function and collective LTG activity is indeed essential for growth and division.[35] The actual physiological function for

100 the majority of LTGs, however, and the reason for their collective essentiality, has
101 remained elusive. Here, we sought to comprehensively illuminate physiological roles for
102 LTGs by extensively characterizing mutants of the Gram-negative pathogen *Vibrio*
103 *cholerae* that are defective for most or all currently annotated LTGs. We find that the vast
104 majority of LTGs is dispensable for growth in laboratory media. Minimal LTG strains are
105 defective for growth in low-salt media and hypersensitive to accumulation of periplasmic
106 sugar polymers. Through analysis of PG turnover products, we show that soluble PG
107 strands accumulate in the wild type and that this is exacerbated in ΔLTG mutants and
108 alleviated by inactivating a major PG endopeptidase. Taken together, our data suggest
109 that lytic transglycosylase activity downstream of PG synthesis mitigates toxic periplasmic
110 accumulation of uncrosslinked, polymeric peptidoglycan turnover products released by
111 endopeptidases.
112
113

114 # Results

115 ***A single LTG is necessary and sufficient for V. cholerae growth***

116 We recently reported that a Δ6 LTG mutant (*rlpA*$^+$ *mltG*$^+$ Δ*mltA* Δ*mltB* Δ*mltC* Δ*mltD* Δ*mltF*
117 Δ*slt70*) was viable under standard laboratory conditions and exhibited only slight
118 morphological defects, including an increase in cell length[35]. Depletion of RlpA from this
119 background resulted in a lethal chaining defect, suggesting that collectively, some degree
120 of LTG activity is essential for *V. cholerae* growth. Since we were previously unable to
121 delete MltG or observe its depletion from a Δ6 LTG background, we asked whether MltG
122 exhibited a synthetic-lethal relationship with the other LTGs. Surprisingly, a quantitative
123 insertion/disruption assay suggested that MltG was fully dispensable in the Δ6 LTG
124 background, so long as essential DNA synthesis genes downstream of *mltG* were
125 expressed *in trans* to ameliorate polar effects of *mltG* disruption (**Fig. 1a, S1ab**). The
126 resulting Δ6 LTG *mltG::kan* mutant was viable in LB but failed to grow in low-salt LB (LB
127 without added NaCl, designated LB0N) (**Fig. S1c**), which could explain why previous
128 attempts to inactivate *mltG* in this background using SacB-based allelic exchange
129 (requiring selection on LB0N+sucrose) were unsuccessful[35]. Consistent with these data,
130 we were then able to generate a clean, viable Δ7 LTG mutant (*rlpA*$^+$ *mltG::stop*
131 Δ*mltABCDF* Δ*slt70*) using a MqsR toxin-based allelic exchange system[37]. The Δ7 mutant
132 sacculus contained only a tenth of the AnhMurNAc residues observed in the wild type
133 sacculus (**Fig. S1d, Tables S1,S2**), suggesting that no highly active LTGs remain in this
134 background. Compared to Δ6 LTG[35], RlpA depletion was more severe in the Δ7
135 background, both by morphology and plating efficiency (**Fig. 1b, Fig. S2**), consistent with
136 Δ7 exhibiting more limited LTG activity than Δ6.

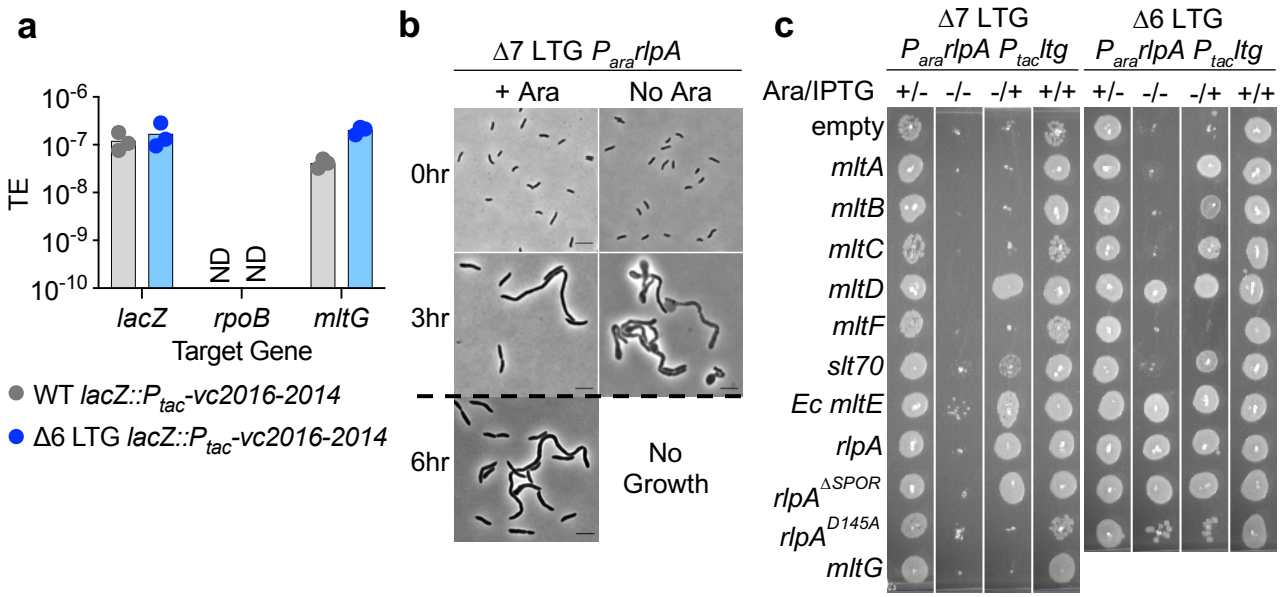


**Figure 1. A single LTG is necessary and sufficient for *V. cholerae* growth and envelope homeostasis**

**(a)** *Trans* expression of DNA synthesis genes *vc2016-2014* permitted pAM299 disruption of native *mltG* locus. *lacZ* and *rpoB* were targeted as positive and negative controls for disruption, respectively. TE = Transformation Efficiency. ND = below limit of detection. 3 biological replicates are shown. **(b)** RlpA was depleted from the WT, Δ6, and Δ7 LTG backgrounds by placing its native promoter under control of arabinose induction and growing from a $10^{-3}$ overnight culture dilution into 5mL LB +/- 0.4% arabinose (ara) at 37 °C with shaking for 3 hrs, back-diluting $10^{-3}$ into fresh media, and incubating for another 3 hrs. Cells were imaged on LB agarose pads. Scale bars = 5μm. Dotted line indicates $10^{-3}$ back-dilution. **(c)** Arabinose-dependent RlpA depletion in Δ6 and Δ7 LTG backgrounds was rescued with IPTG-inducible LTGs by growing cultures in LB +/- ara (0.4%) and +/- IPTG (200μM) in 96 well plates at 37 °C without shaking for 3hrs, back-diluting $10^{-3}$ into fresh media, incubating another 3 hrs, and spotting directly onto the same media +kan50. Plates were incubated at 30 °C for 24hrs before imaging. Complete plating efficiencies associated with panels (B) and C) can be found in Fig. S2 and S4. Images are representative of 3 biological replicates.

Importantly, growth of Δ7 LTG depended on RlpA LTG activity, as $RlpA^{D145A}$, a predicted active site RlpA mutant[34] (**Fig. S3ad**) was unable to promote growth (**Fig. 1c, S4**). Conversely, a mutant in the conserved SPOR domain (which is essential for septal localization in *P. aeruginosa*[34] and *V. cholerae*, **Fig. S3c**, but not for LTG function) fully

160 complemented both Δ6 and Δ7 **(Fig. 1c, S4)**, suggesting that RlpA LTG activity, but not
161 septal localization, are essential in these backgrounds. Taken together, these results
162 demonstrate that at least during growth in standard laboratory conditions, *V. cholerae*
163 only requires one active LTG of the 8 currently annotated in its genome.
164
165 ***Only a subset of LTGs can independently fulfill all essential LTG functions***
166 Since RlpA LTG activity, but not septal localization, was essential for Δ6 and Δ7 growth,
167 we asked whether growth required specialized LTG function, or just PG cleavage function
168 in general. To test this, we assessed the ability of other LTGs to complement Δ6 and Δ7
169 (**Fig. 1c, S4**). Only two native LTGs, MltD and Slt70, could fully (MltD) or partially (Slt70)
170 substitute for RlpA in the Δ7 LTG background, demonstrating that RlpA, MltD, and (to a
171 lesser degree) Slt70 are the only *V. cholerae* LTGs capable of fulfilling all required LTG
172 roles. Additional LTGs, MltA, MltB, and MltC, were able to rescue RlpA depletion in the
173 Δ6 LTG background (where MltG is present), but not the Δ7 LTG background (where MltG
174 is absent). These observations suggest that LTGs perform at least two separable
175 essential functions for viability, where MltG can perform one function but requires MltA,
176 MltB, or MltC to perform another, and vice versa, as none of these LTGs are
177 independently capable of supporting growth. Intriguingly, the *E. coli* LTG MltE, for which
178 *V. cholerae* has no known homologue, was also capable of fully supporting *V. cholerae*
179 growth as the sole functioning LTG, suggesting that LTG essential functions may not
180 depend on specific protein-protein interactions. Collectively, these data suggest that
181 LTGs are partially redundant; but some LTGs also exhibit varying degrees of functional
182 specificity.

183

184 ***LTGs are required during vegetative growth***

185 We were surprised that our strains lacking major LTG activity (even Δ7) were viable. We
186 thus sought to characterize growth and morphology of these backgrounds in more detail.
187 While the Δ6 and Δ7 mutants grew at wild-type growth rates in LB medium when cultures
188 were started from a 100-fold dilution of saturated overnight cultures, we noticed a dilution-
189 dependent exacerbation of growth and morphology defects **(Fig. 2, S5, S6)**. When Δ7
190 LTG cultures were highly diluted from overnight cultures to increase the number of
191 generations spent in exponential growth, we started to observe a marked growth defect
192 (**Fig. 2ab, S6a**). Conversely, the *mltG::stop* single mutant and Δ6 LTG mutant grew at
193 wild-type growth rates independent of initial dilution factor (**Fig. 2b, S6a**). These data
194 suggest an essential or near-essential role for MltG during sustained exponential growth,
195 albeit only when other LTGs are also inactivated. We also observed diverse aberrant
196 morphologies within the LTG-deficient mutants (but not a Δ*mltG*::stop single mutant)
197 under these conditions (**Fig. 2c, S5**). Interestingly, despite lacking most members of an
198 entire class of PG enzymes, Δ6 and Δ7 only exhibited only mild defects in length and
199 width homeostasis (**Fig. 2de**, **Fig. S6**), which were only dilution-factor dependent for cell
200 length (suggesting a cumulative division defect). When we followed a time-course after
201 back-dilution from stationary phase, we observed morphological defects accumulating in
202 exponential phase and then largely disappearing in stationary phase (**Fig. S7**) in both Δ6
203 and Δ7. Collectively, these observations suggest that LTG-deficient mutants suffer from
204 cumulative damage during exponential growth, which is partially alleviated in stationary
205 phase.

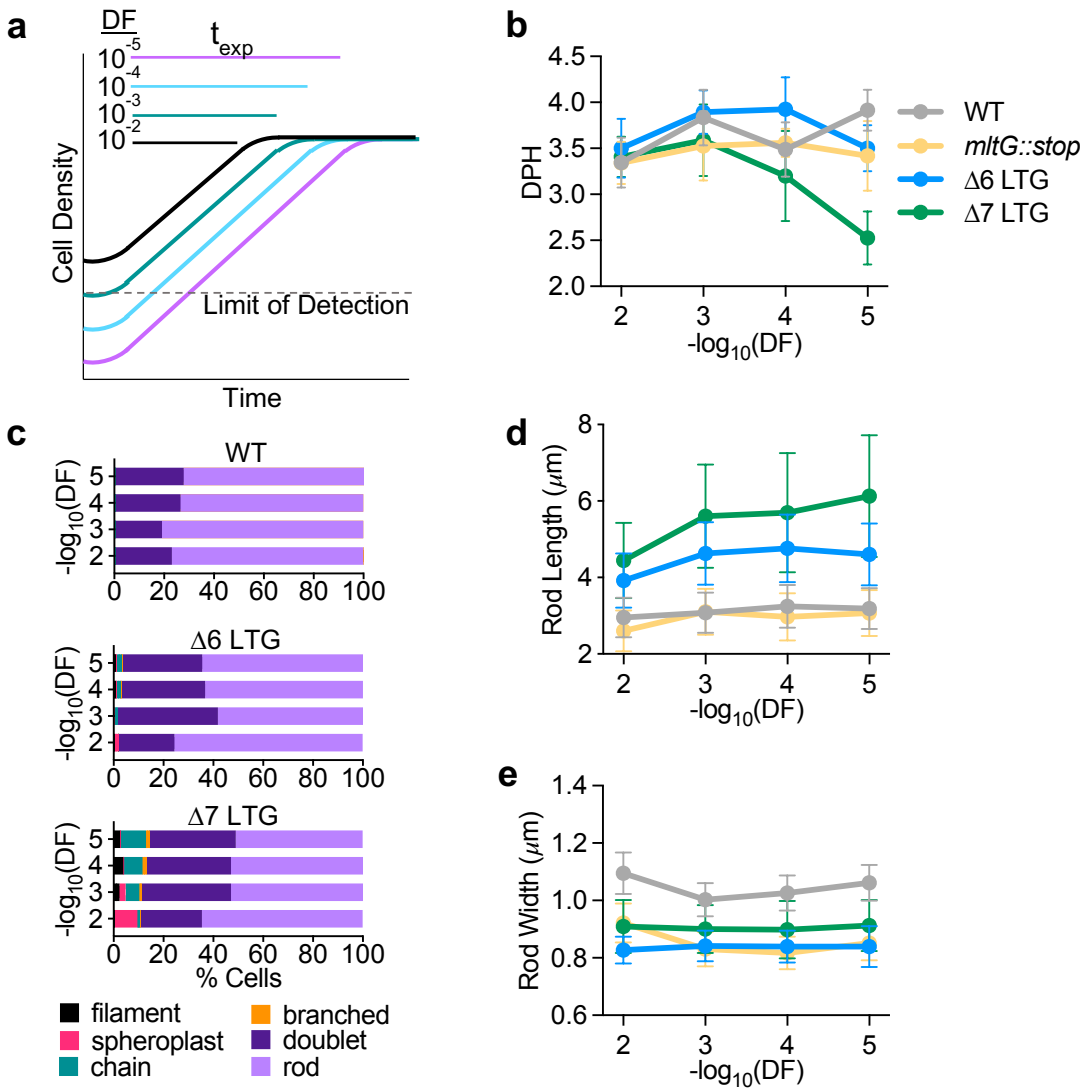


**Figure 2. LTG insufficiency causes cumulative growth and morphology defects**
**(a)** Schema describing relationship between dilution factor (DF) of saturated cultures into fresh media and time spent in exponential growth ($t_{exp}$). **(b)** Mass doubling times (doublings per hour, DPH) from growth curves performed in LB inoculated with 10-fold serial dilutions of saturated overnight cultures. Values were calculated from growth curves shown in Fig. S6. Error bars represent standard deviation of the mean, n≥3. **(c)** Relative abundance of cell morphologies from cultures at $OD_{600}$ 0.3 from panel C. n>500 cells. Definition criteria and images are shown in Fig. S5. Mean length **(d)** and width **(e)** as a function of dilution factor (DF) of rod cells from panel (C). n>500 rods.

219 ***LTG activity is required for survival in hypo-osmotic conditions***

220 Our results detailed above suggested that the majority of LTGs are dispensable for
221 growth, catalyzing renewed interest in the question of what their physiological roles are.
222 To dissect potential roles for LTGs in cell envelope integrity maintenance, we subjected
223 the Δ6 and Δ7 mutants to low osmolarity challenge. Similar to the morphology and growth
224 defects in LB (**Fig. 2**, **S5 – S7**), both mutants were sensitive to low salt conditions in a
225 dilution-dependent manner (**Fig. 3a, S8a**). Interestingly, the Δ7 LTG mutant grew at wild-
226 type rate during the initial growth period before onset of lysis, suggesting that it is not the
227 initial shock of changing osmotic conditions that kills this mutant, but rather some
228 cumulative damage during growth in low-salt conditions (**Fig. 3a, S8a**). Importantly, this
229 rules out a simple cell envelope defect as a cause of LTG-deficient mutant osmo-
230 sensitivity. We then sought to dissect the contributions of individual LTGs to salt
231 sensitivity. Other than RlpA, which has an established role in LB0N growth[34,35] and is still
232 present in the Δ6 and Δ7 mutants, no other single LTG mutant exhibited a strong growth
233 defect in LB0N (**Fig. S9a**), all suggesting that this defect is an accumulative function of
234 collective LTG insufficiency. Several LTGs (MltA, MltB, Slt70, and EcMltE) were able to
235 rescue Δ6 LTG growth in LB0N at higher dilutions (**Fig. S9c**), but none could rescue Δ7
236 growth in LB0N except MltG, which only partially restored growth to Δ6 mutant levels (**Fig.
237 S9d**). This suggests that no single LTG is be able to fully support growth in LB0N, and
238 that MltG, despite not exhibiting a defect as a single mutant, is particularly important in
239 this environment when other LTGs are inactivated. Intriguingly, overexpression of *mltF*
240 was toxic for both the Δ6 (LB0N only) and the Δ7 mutant (LB) (**Fig. S9bcd**), preventing
241 us from assessing its potential for LTG-deficient mutant complementation.

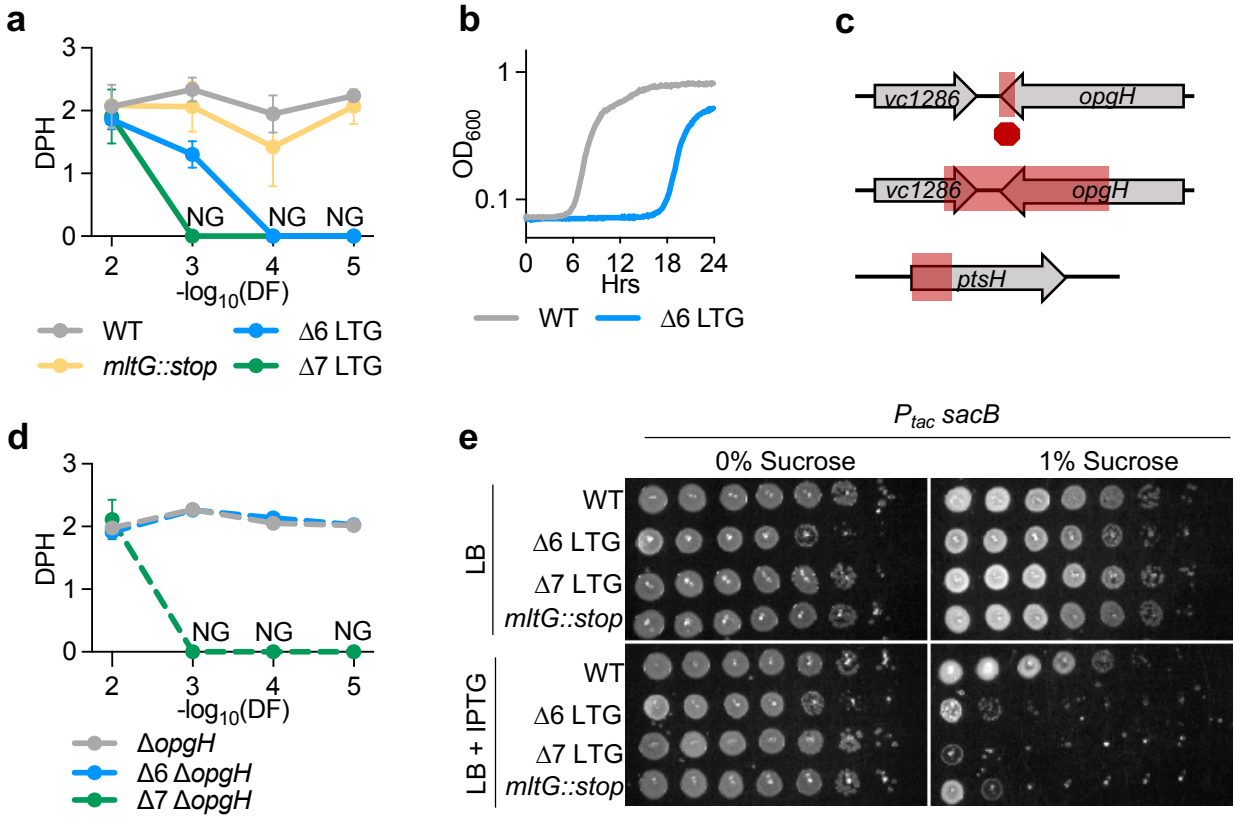


**Figure 3. LTG mutants are hypersensitive to low osmolarity and accumulation of periplasmic polymers**

**(a)** Mass doublings (doublings per hour, DPH) upon increasing dilutions (DF, dilution factor) during growth in LB0N. Values were calculated from growth curves in Fig. S8A. Error bars represent standard deviation of the mean, n≥3. NG, no growth **(b)** Representative growth curve in LB0N showing late-growing spontaneous suppressor in Δ6 LTG **(c)** Whole genome sequencing of Δ6 LB0N suppressor mutations identifies a premature stop resulting in a 6% 3' truncation of *opgH;* a deletion resulting in a 56% 3' truncation of *opgH* and 36% 3' truncation of *vc1286;* and a deletion of the 5' end of *ptsH*. **(d)** Validation of low osmolarity growth defect suppression by an *opgH* mutation. Shown are mass doublings (doublings per hour, DPH) upon increasing dilutions (DF, dilution factor) during growth in LB0N. Values were calculated from growth curves shown in Fig. S8E **(e)** Saturated overnight cultures harboring IPTG-inducible *sacB* were 10-fold serially diluted and plated on LB+kan50 +/- 200μM IPTG +/- 10% sucrose, incubated at 30 °C, and imaged 24 hrs before. Representative of 3 biological replicates. Empty vector and LB0N controls are shown in Fig. S11.

262 ***LTG mutants are hypersensitive to accumulation of periplasmic polysaccharides***

263 To determine the reason for ΔLTG defects in low salt media, we took advantage of the
264 spontaneous appearance of suppressors arising during Δ6 LTG growth in LB0N. (**Fig. 3b,**
265 **Fig. S8**). Whole genome sequencing of three stable suppressors identified three unique
266 mutations: a deletion in *ptsH* (*vc0966*), a frameshift mutation in *opgH* (*vc1287*), and a
267 deletion mutation affecting both *opgH* and a downstream gene (*vc1286*) (**Fig. 3c**). *ptsH*
268 encodes HPr, a key regulator of sugar import via the phosphoenolpyruvate-carbohydrate
269 phosphotransferase system (PTS).[38] OpgH is critical to the synthesis of periplasmic
270 glucans (OPGs), which accumulate under conditions of low osmolarity and have been
271 implicated in a variety of cell functions, including steady-state maintenance of osmolarity
272 in the periplasm.[39] We were particularly intrigued by the role of periplasmic glucans and
273 validated restoration of Δ6 LTG LB0N growth using clean deletion mutants. Inactivation
274 of *opgH* completely restored wild-type growth of the Δ6 LTG mutant in LB0N, independent
275 of initial dilution factor (**Fig. 3d, S8e**). In contrast, inactivation of *opgH* was only able to
276 restore growth of the Δ7 LTG mutant in LB0N from a $10^{-2}$ inoculum (**Fig. 3d**, **Fig. 8e**), but
277 not from greater dilutions, nor from a $10^{-5}$ inoculum in LB (**Fig. S8cd**), indicating that the
278 Δ7 LTG mutant has additional exponential growth-dependent defects unique from the Δ6
279 LTG mutant. Interestingly, OpgH orthologues in *E. coli* and *Y. pseudotuberculosis* have
280 also been ascribed a moonlighting function, tying carbon availability with cell length by
281 inhibiting FtsZ filamentation when UDP-glucose levels are high in the cell[40,41]. The
282 elongated cell phenotype of the Δ6 LTG and Δ7 LTG mutants could in principle be
283 indicative of a similar activity by *V. cholerae* OpgH; however, deleting *opgH* from the Δ6
284 LTG mutant did not restore wild-type cell length in Δ6 (**Fig. S10a**). Additionally, alignment

285 of *V. cholerae* OpgH with *E. coli* and *Y. pseudotuberculosis* suggests that it lacks much
286 of the N-terminal domain that was shown to interact with FtsZ in *E. coli* (**Fig. S10b**).[40]
287
288 We consequently considered a model where accumulation of periplasmic glucans is
289 detrimental to ΔLTG mutants, e.g., via periplasmic crowding or an increase in periplasmic
290 osmolarity. To test this model, we used an unrelated system to increase periplasmic
291 crowding. The *B. subtilis sacB* gene product isomerizes and polymerizes sucrose
292 monomers into levan molecules up to several kD[42], molecules much too large to escape
293 the gram-negative periplasm through outer membrane porins. This is often exploited in
294 allelic exchange methods for mutant generation as a means of counterselection,[43-45]
295 where, for example, WT *V. cholerae* is sensitive to *sacB* expression in LB0N+sucrose.
296 We hypothesized that the ΔLTG mutants might be hypersensitive to levan accumulation
297 even in standard LB salt conditions (1% W/V). To test this, we engineered strains
298 overexpressing *sacB*. Consistent with the use of *sacB* as a counterselection method
299 under low salt conditions, the wild type is sensitive to *sacB* induction on LB0N (**Fig. S11**),
300 but not LB. In contrast, we observed a *sacB*-dependent plating defect on sucrose in the
301 Δ6 and Δ7 LTG mutant on LB (**Fig. 3e, S11**). Interestingly, the *mltG::stop* mutant also
302 exhibited hypersensitivity to SacB activity (**Fig. 3e, S11**), suggesting that accumulating
303 MltG substrate is a particularly strong direct or indirect contributor to this phenotype.
304 Collectively, our data suggest that ΔLTG mutants suffer from either hyperosmotic stress
305 or excessive molecular crowding in the periplasm, which can be exacerbated through the
306 induction of long-chain polysaccharides.
307

308 ***PG transglycosylase activity causes Δ6 LTG mutant periplasmic stress***

309 Based on our model that accumulation of polysaccharides in the periplasm is toxic, we
310 predicted that induction of "futile cycling" (accumulation of uncrosslinked PG strands
311 caused by uninterrupted GT activity during TP inhibition, e.g. by β-lactams[46]) should
312 exacerbate LTG-deficient mutant sickness, and this has indeed been shown with Slt70 in
313 *E. coli*[46]. To test this hypothesis, we assessed susceptibility of ΔLTG mutants to cell wall-
314 acting antibiotics with varying ability to induce futile cycling. In a disk diffusion assay, the
315 Δ6 and Δ7 LTG mutants were hypersensitive to inducers of futile cycling, i.e., general
316 PBP inhibition by Penicillin G as well as to inhibition of specific PBPs including PBP3
317 (aztreonam), PBP2 (mecillinam), and PBP1b (cefsulodin) (**Fig. 4a**). Conversely, both the
318 Δ6 and the Δ7 mutant exhibited wild-type sensitivity to moenomycin and fosfomycin, both
319 of which inhibit cell wall synthesis without inducing futile cycling. Thus, β-lactam sensitivity
320 of LTG-deficient mutants is not necessarily tied to simple inhibition of cell wall synthesis,
321 but potentially also to periplasmic crowding due to the accumulation of uncrosslinked PG
322 strands. Curiously, the Δ7 LTG mutant was hypersensitive to MreB inhibition by MP265.
323 This suggests that in the absence of other LTGs, MltG contributes to survival upon Rod
324 system insufficiency through an unknown mechanism.

325

326

327

328

329

330

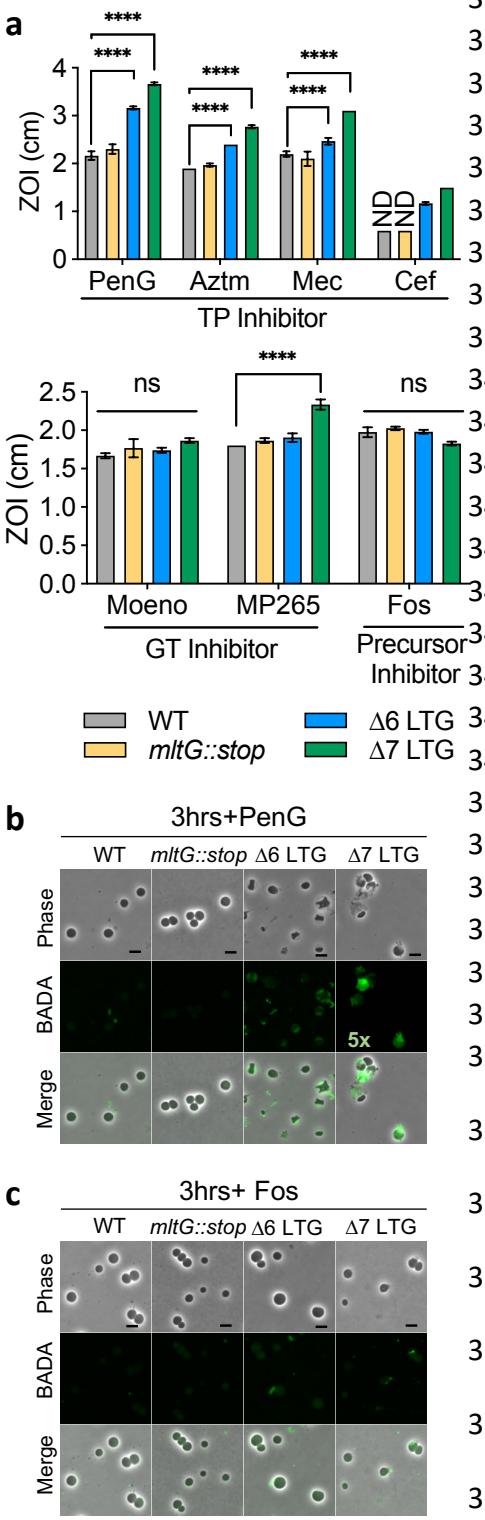


**Figure 4. LTG mutants are hypersensitive to antibiotics promoting periplasmic PG accumulation**

**(a)** Sensitivity to Penicillin G (PenG), aztreonam (AZTM), mecillinam (Mec), cefsulodin (Cef), moenomycin (Moeno), MP265, and Fosfomycin (Fos) measured as Zone of Inhibition (ZOI) in a disk diffusion assay. ND = No ZOI around disk. Error bars = standard deviation. Significance determined by one-way Anova. ns = p>0.05, * = p< 0.05, ** = p<0.01, *** = p<0.001, **** = p<0.0001. Overnight cultures were diluted 1:100 into LB+BADA (100μM) and grown at 37°C to $OD_{600}$ 0.5 before addition of **(b)** PenG (100μg $ml^{-1}$) or **(c)** Fosfomycin (500μg $ml^{-1}$). Samples were washed and imaged after 3hrs of antibiotic exposure. Fluorescence was normalized to the same intensity threshold for comparison except where indicated (Exceptionally bright samples were normalized to a higher intensity threshold denoted by the multiplier). Representative of 2 biological replicates. Scale bar = 5μm

To further dissect PG strand accumulation under these conditions, we visualized the fate of PG during antibiotic treatment using the cell wall label BADA.[47,48] The Δ6 and Δ7 LTG mutants were all readily labeled when grown with BADA (**Fig. S12, S13**) prior to antibiotic addition. After 3 hours of treatment with Penicillin G (100μg $ml^{-1}$, 20xMIC), the Δ6 and Δ7 LTG mutants accumulated strong periplasmic BADA signal compared to the

365 wild-type spheroplasts in which the cell wall is presumably completely degraded (**Fig. 4b**).
366 At earlier stages of penicillin treatment, it also appeared that the Δ6 and Δ7 LTG mutants
367 were slower to degrade their rod-shaped poles (**Fig. S12**). Treatment with fosfomycin
368 (500μg $ml^{-1}$) did not result in pronounced BADA accumulation in the periplasm,
369 suggesting that this signal does not reflect sacculus degradation, but indeed relies on
370 ongoing cell wall synthesis (i.e., futile cycling) (**Fig. 4b, S13**).
371
372 ***LTG insufficiency results in periplasmic PG strand accumulation***
373 Why are LTG mutants sensitive to periplasmic accumulation of polymers? Accumulating
374 PG debris released during PG synthesis could, in principle, increase periplasmic
375 osmolarity and/or crowding, explaining defects associated with low salt conditions and
376 periplasmic polysaccharide accumulation. We therefore sought to quantify soluble,
377 periplasmic PG debris within crude cell lysates (excluding PG released into the growth
378 medium). Canonical PG architecture analysis relies on SDS-boiled sacculi isolated by
379 ultra-centrifugation, which permits sacculus characterization (**Fig. S1d**), but ignores
380 solubilized, uncrosslinked (freely-diffusing) PG fragments associated with PG turnover
381 processes such as those potentially mediated by LTGs. We thus analyzed fragments that
382 remained soluble after sedimentation of purified sacculi, i.e., PG material that freely
383 accumulates within the periplasm (or inside the cell) but is not attached to the cell wall.
384 Since entire periplasmic PG strands cannot be easily resolved using subsequent LC-MS
385 analysis, we also digested the soluble PG fraction with muramidase (to generate smaller
386 monomers suitable for LC-MS detection) and then compared muramidase-treated vs.
387 untreated traces to determine soluble PG architecture **(Fig. 5a)**. We first analyzed soluble

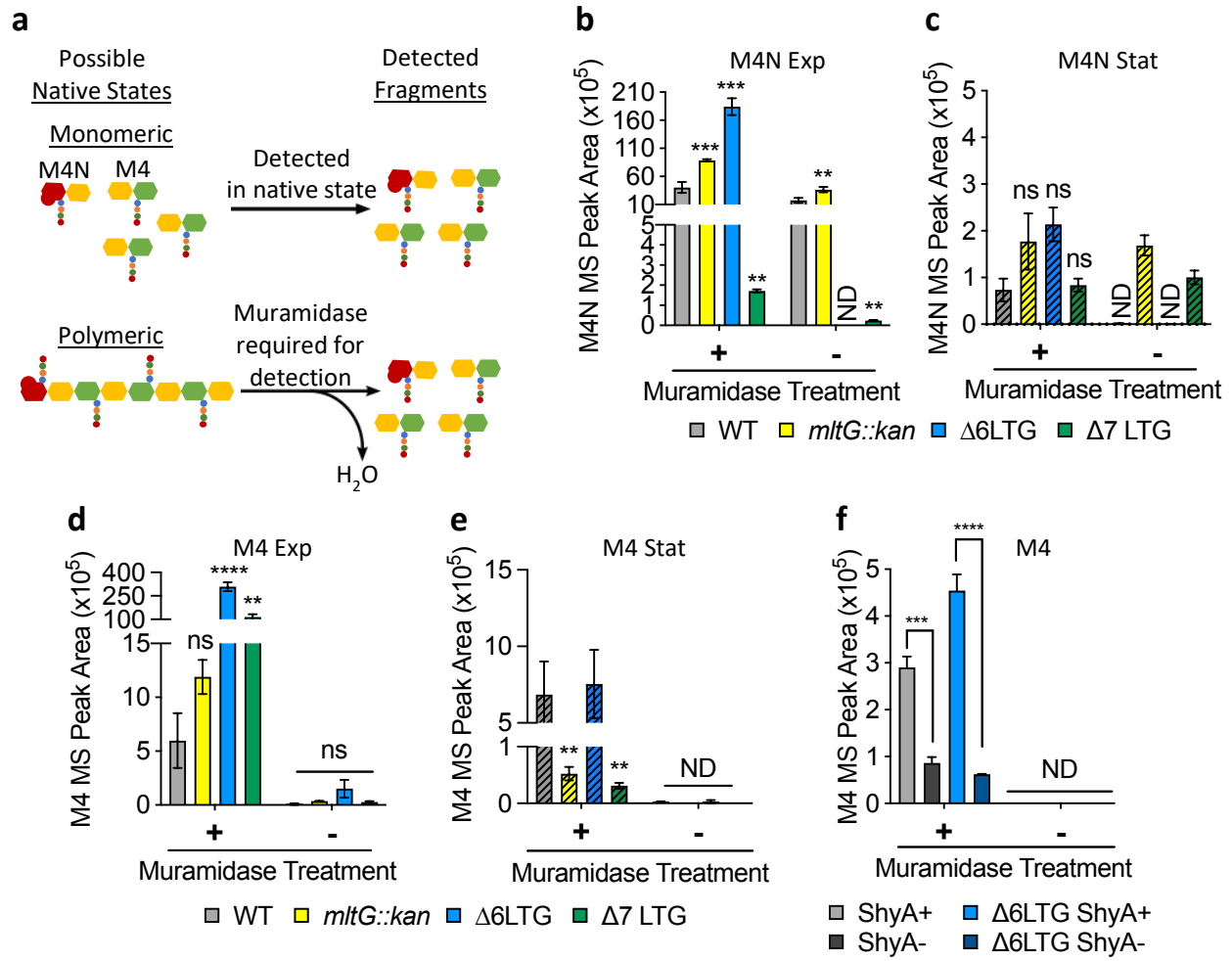


**Figure 5. Periplasmic uncrosslinked PG strands accumulate in an endopeptidase-dependent manner during normal growth**

**(a)** Schema describing muramidase-treatment dependence of detection of monomeric or polymeric PG fragments. M4N = anhMurNAc-tetrapeptide. M4 = reduced MurNAc-tetrapeptide. **(b-e)** Overnight cultures of. WT and ΔLTG mutants were diluted 1:100 into LB, grown at 37°C, and harvested at $OD_{600}$ 0.3 (Exp, solid bars) and 1.2 (Stat, striped bars) for soluble PG analysis by LC-MS. MS peak areas for M4N and M4 are shown here. Means compared to WT by unpaired t-tests, n=3. **(f)** WT and Δ6 LTG strains harboring a single chromosomal copy of *shyA* under an IPTG-inducible promoter were grown from $10^{-2}$ inocula for 3hrs ($OD_{600}$ ~1.0) in LB with (ShyA+) or without (ShyA -) 200μM IPTG at 37 °C and harvested for soluble PG analysis by LC-MS. Means compared by unpaired t-test, n=3. All error bars = standard deviation. ns = p>0.01, ** = p<0.01, *** = p<0.001, **** = p<0.0001. ND = Not detected in all replicates.

402 products of LTG activity (**Fig. 5bc, Table S3-S6**). AnhMurNAc-tetrapeptide (M4N) was
403 abundant in the wild type during exponential phase, and predictably, M4N was
404 significantly depleted in the Δ7 LTG soluble muropeptide profile. Surprisingly, M4N was
405 enriched in the *mltG::kan* and Δ6 LTG mutants, suggesting that the absence of some
406 LTGs might cause upregulated activity of others.
407
408 Importantly, MurNAc-tetrapeptide species without anhMurNAc (M4) were detectable in
409 the WT during exponential phase, and significantly enriched in the Δ6/Δ7 LTG mutants
410 (**Fig 5d, Tables S3-S6**). By comparing the muramidase-treated vs. untreated samples,
411 we can infer the native state of these M4 and M4N (**Fig. 5abd**), i.e., determine whether
412 these species occur predominantly as monomers or as parts of PG polymers *in vivo*. Both
413 species were significantly depleted in the muramidase-untreated samples, suggesting
414 that *in vivo*, they are part of polymeric, uncrosslinked peptidoglycan strands. It is important
415 to note that M4 monomers are not intermediates of cell wall synthesis (which proceeds
416 from a tripeptide directly to pentapeptide due to addition of preformed D-Ala-D-Ala
417 dipeptide).[49] This, in conjunction with a strong muramidase-treatment-dependence of the
418 abundance of M4 excludes a cytoplasmic origin of this species. It is also interesting to
419 note that, unlike the WT, *mltG::kan*, and even Δ6 LTG mutant, the Δ7 LTG appears to
420 have a disproportionately large pool of polymeric M4 species (muramidase-dependent)
421 compared to M4N species, suggesting that either the soluble PG strands in the Δ7 LTG
422 mutant are extremely long, or perhaps do not ubiquitously terminate in anhMurNAc
423 residues. The abundance of soluble PG strands decreased in stationary phase (**Fig. 5ce,**
424 **Tables S3-S6**), which suggests that in the LTG-deficient mutants, these strands are

425 somehow cleared by RlpA, an unrecognized LTG, or a cryptic PG hydrolase. Reduction
426 of these uncrosslinked strands in stationary phase is consistent with the alleviation of
427 morphology defects observed as cells exit exponential growth **(Fig. S7)**.
428
429 We next asked how these polymeric uncrosslinked PG strands might be generated. Since
430 endopeptidases have been suggested to be essential for sacculus expansion during cell
431 elongation, we hypothesized that these soluble strands may reflect endopeptidase
432 activity, which would imply that EPs do not simply relax PG crosslinking (as commonly
433 assumed), but also might excise entire strands that accumulate - at least transiently - in
434 the periplasm. To test this hypothesis, we depleted the major housekeeping EP ShyA[50]
435 from a Δ6 LTG mutant, and found that the most abundant monomer species, M4, was
436 reduced in a ShyA-dependent manner in both the WT and Δ6 LTG mutant (**Fig. 5f, Tables**
437 **S7, S8**). This strongly suggests that ShyA produces the majority of the uncrosslinked
438 strands in the periplasm. Curiously, depletion of ShyA in the Δ6 LTG background resulted
439 in large, irregular cells (**Fig. S14**), suggesting a cell envelope defect upon EP
440 insufficiency. Additionally, ShyA was required for Δ6 LTG mutant colony formation on LB
441 plates, but Δ6 LTG liquid cultures depleted for ShyA remained viable and could be
442 rescued on plates restoring *shyA* expression (**Fig. S14**). Altogether, the data suggest that
443 EPs excise entire PG strands that accumulate in the periplasm until they are later cleared
444 by LTGs.
445
446
447

448 ## Discussion

449 The exact contributions of LTGs to cell growth have remained elusive, mainly due to the
450 high level of apparent redundancy of these enzymes, which hampered classical
451 genotype-phenotype association analyses. While circumstantial evidence abounds, no
452 collective physiological characterization of essential LTG function has been conducted in
453 any organism, and even cases of demonstrated synthetic lethal relationships are rare and
454 rely on indirect evidence (inability to delete LTG genes).[33,51,52] The *V. cholerae* Δ6 and Δ7
455 LTG mutants described here provide a vital platform for exploring both the collective and
456 individual contributions of lytic transglycosylases to bacterial viability.

457

458 ***Conserved LTGs are not functionally equivalent***

459 In this study we confirm that LTG enzymatic activity is essential for growth and division.
460 We further demonstrate that some functional redundancy exists in *V. cholerae* between
461 diverse LTG families, as has been observed in other bacteria [12,20,53]. Members of LTG
462 families 1A (Slt70), 1D (MltD) and 6A (RlpA) can support growth independent of all other
463 natively encoded LTGs from families 1B, 1E, 2A, 3A, and 5A. Certain *V. cholerae* LTGs
464 additionally exhibit complementary genetic relationships in the absence of all other LTGs,
465 implying there are at least two essential roles for LTGs. For example, while neither MltG,
466 MltA, MltB, nor MltC can support growth on their own, strains expressing the MltG+MltA,
467 MltG+MltB, or MltG+MltC pairs are each viable. Surprisingly, and importantly, essential
468 LTG activities may not require conserved protein-protein interactions as suggested by the
469 viability of a *V. cholerae* mutant expressing non-native *E. coli* MltE as its sole LTG.
470 Scheurwater and Clarke unsuccessfully but informatively attempted to inactivate *mltF* in

471 an *E. coli* Δ6 LTG (Δ*mltABCDE* Δ*slt70*), suggesting that the essentiality of LTG activity is
472 conserved between *E. coli* and *V. cholerae,* and that MltF and MltG may not be
473 functionally redundant in *E. coli*.[52] In contrast, *mltF* inactivation is not synthetically lethal
474 with Δ*mltABCD* Δ*slt70* in *V. cholerae*. In fact, restoring MltF expression in the Δ6 and Δ7
475 LTG background is toxic, indicating that *V. cholerae* and *E. coli* exhibit different genetic
476 relationships between homologs of the same LTGs. This is perhaps most strongly
477 exemplified by the conservation of RlpA in both species, where *E. coli* RlpA has no
478 detectable LTG activity[34], yet *V. cholerae* RlpA can perform essential functions as the
479 sole LTG. Recently, the hydrolytic enzyme DigH in *E. coli* was shown to be functionally
480 similar to LTGs by contributing to the resolution of septal PG during daughter cell
481 separation[54]. The activity of DigH (of which *V. cholerae* does not possess a strong
482 homolog) may explain why *E. coli* does not appear to require RlpA LTG activity; this LTG-
483 like physiological role for a hydrolytic enzyme also suggests that we may need to look
484 beyond LTGs to fully address the roles for glycosidic bond cleavage within PG.
485
486 The functional redundancy of LTGs is also likely the root of an apparent paradox. Release
487 of new PG strands from undecaprenyl pyrophosphate should be an essential function, as
488 anchoring of PG to the inner membrane is toxic[55] and is likely necessary for lipid carrier
489 recycling. Yet MltG, the highly conserved "PG terminase" that associates with PG
490 synthetic complexes to release new strands, is not essential. MltG can be inactivated in
491 wild type *V. cholerae* without significant consequence but our Δ7 LTG (*mltG*-null) mutant
492 lost viability upon sustained growth in exponential phase in LB. It is therefore likely that
493 other LTGs can partially complement for terminase activity. The dilution-dependent Δ7

494 LTG growth defect further suggests that either RlpA has at least partial terminase activity
495 and/or that during brief growth in exponential phase, terminase activity is non-essential.
496 MltG essentiality (or near-essentiality) can thus perhaps only be appreciated in a multiple
497 LTG background under conditions where terminase activity is expected to be most
498 important. This is also evidenced by the increased sensitivity of the Δ7 LTG mutant to
499 hypo-osmotic conditions that cannot be rescued via the same mechanisms that rescue
500 Δ6 LTG mutant, i.e., inactivation of OPG synthesis, as well as hypersensitivity to MreB-
501 inhibitor MP265. All of these defects point to a unique, MltG-dependent, conditionally
502 essential LTG function.
503
504 ***LTGs manage the periplasmic environment***
505 By analyses of soluble PG, we discovered that even wild-type *V. cholerae* accumulates
506 loose strands of uncrosslinked PG of periplasmic origin (detected as muramidase-
507 dependent, soluble M4 products) and that production of these strands is dependent on
508 the EP ShyA. PG strands appear to accumulate to detrimental levels in the Δ6 and Δ7
509 mutants and we thus propose that processing soluble PG is a major collective function of
510 LTGs. PG strand accumulation induces hypersensitivity to other polymeric sugars in the
511 periplasm, such as OPGs, SacB-generated levans and β-lactam-induced futile cycling
512 products. This polysaccharide toxicity may arise from the fact that these large polymers
513 (PG, OPGs, or levans) cannot diffuse out through OM porins, accumulating in a growth
514 and/or substrate-dependent manner. This would inappropriately increase the osmolarity
515 and/or cause excessive crowding[5] of the periplasm to interfere with normal growth-related

516 processes, as exemplified by the mild division defect of the *V. cholerae* LTG-deficient
517 mutants.
518
519 ***Broader implications for LTGs in PG dynamics***
520 Our data suggest that the most important roles for LTGs may not include "making space"
521 for new PG insertion, as has been assumed for fundamental models of PG synthesis.
522 More likely, LTGs clear the periplasm of most PG debris generated by endopeptidases
523 during normal growth by facilitating either recycling or release of small fragments into the
524 environment (**Fig. 6**). As such, this collectively essential function of LTGs may not be tied
525 to a direct influence on PG synthesis. Importantly, uncrosslinked strands are not a deviant
526 feature unique to the LTG-deficient mutants nor β-lactam treatment (though they become
527 more apparent under these conditions), as they were also detectable in the wild type
528 during normal growth. Detection of EP-dependent, uncrosslinked PG strands suggests
529 that EP activity might be temporally separated from LTG-mediated turnover of those PG
530 strands. This is seemingly contrary to pervasive models proposing a synchronized
531 synthetic/autolytic complex that digests old PG while simultaneously building new PG. If
532 such a complex exists, LTGs collectively maintain an important role complementary to it,
533 but not inevitably as part it.

534

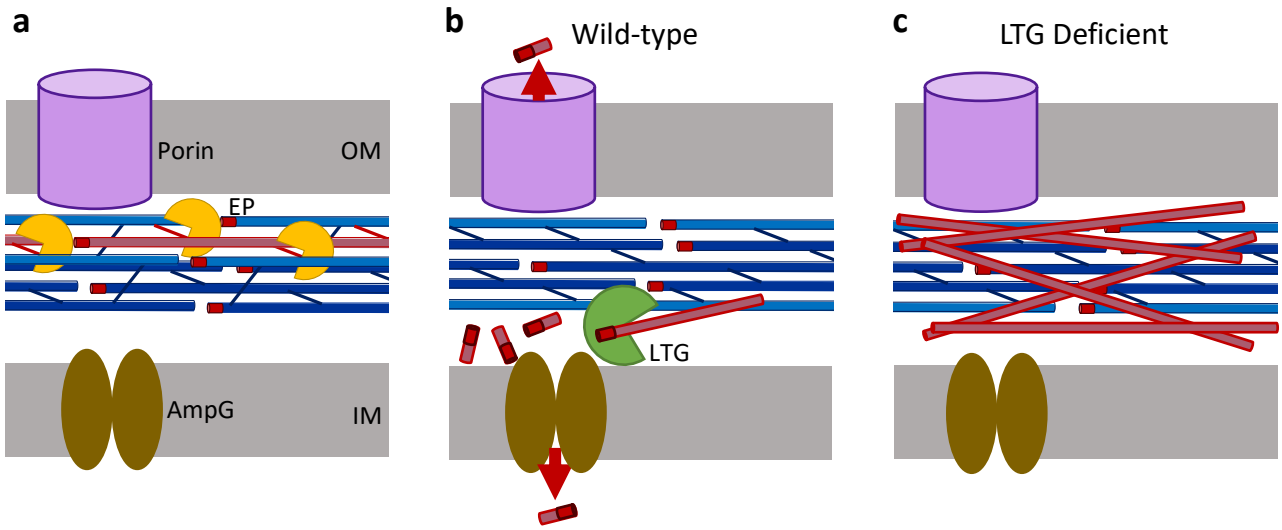


535 **Figure 6. Model for LTG-mediated removal of toxic PG debris**
536 **(a)** Endopeptidases (EPs, Yellow) excise PG strands (Red) from the sacculus (Blue),
537 permitting sacculus expansion. **(b)** In wild-type cells, lytic transglycosylases (LTGs,
538 Green) digest excised, uncrosslinked PG strands into smaller fragments that can be
539 recycled by AmpG (Brown) or released through porins (Violet) **(c)** In LTG deficient cells,
540 excised PG debris crowds the periplasm and becomes toxic
541

542 Lastly, while high accumulation of PG strands is toxic, maintaining a small pool of
543 uncrosslinked PG material may actually serve a beneficial purpose to cells under some
544 conditions; bacteria might thus have an adaptive reason for avoiding tightly coordinating
545 LTG activity with synthesis. Inactivation of *sltY* in *E. coli,* for example, can promote β-
546 lactam resistance by upregulating L,D-crosslinking activity of L,D-transpeptidase LdtD
547 (YcbB), presumably due to the increased presence of uncrosslinked glycan strands under
548 these conditions.[64] It is possible that one function of L,D-TPs is to patch holes in the
549 sacculus via readily available soluble PG strands, constituting an innate "bike tire repair
550 kit" for the bacterial cell wall. Future studies of this LTG-mediated turnover of
551 uncrosslinked PG could be critical for understanding PG repair mechanisms, as well as
552 general periplasmic homeostasis, both of which have been historically elusive topics.

553

554 ## Methods

555 ***Bacterial strains and growth conditions***

556 *V. cholerae* strains in this study are derivatives of *V. cholerae* WT El Tor strain N16961
557 [65]. Construction of plasmids and mutant *V. cholerae* strains is described in the next
558 section along with a table of strains and plasmids used in this work (**Tables S9-S11**).

559

560 Strains were grown at 30°C or 37°C in Luria-Bertani (LB, Fisher Bioreagents# BP97235)
561 with or without 1% NaCl, 1% sucrose, or 10% sucrose, or in M9 minimal media + 0.4%
562 glucose (Cold Spring Harbor Protocols) where indicated in the figure legends. Growth
563 media were supplemented with kanamycin (50 µg $ml^{-1}$), ampicillin (25 µg $ml^{-1}$), or
564 chloramphenicol (5 µg $ml^{-1}$) in plates and overnight cultures when needed to maintain
565 plasmids or chromosomal integration of suicide vectors. Genes under $P_{ara}$ and $P_{tac}$
566 regulation were induced with 0.4% L-arabinose or 200 µM isopropyl-β-D-1-
567 thiolgalactopyranoside (IPTG), respectively.

568

569 ***Construction of plasmids and strains***

570 A summary of all strains, plasmids, and primers used in this study can be found in Tables
571 S9-S11. *E. coli* DH5α λ*pir* was used for general cloning, while *E. coli* SM10 or MFD λ*pir*
572 were used for conjugation into *V. cholerae*[66]. Plasmids were constructed using Gibson
573 assembly[67] with the exception of plasmids expressing *rlpA*Δ*SPOR* or *rlpA*$^{D145A}$, which
574 were generated by site directed mutagenesis of the parent wild-type sequence *rlpA*
575 plasmids. All Illumina whole genome sequencing and variant calling for Δ6 LTG and Δ7

576 LTG strain verification or suppressor identification was performed by the Microbial
577 Genome Sequencing Center (MiGS, Pittsburg, PA, USA).
578
579 Most chromosomal in-frame deletions (or premature stop codon mutants) were generated
580 using the pCVD442 *ampR/sacB* allelic exchange system[68]. 500bp regions flanking the
581 gene to be deleted were amplified from N16961 genomic DNA by PCR, cloned into
582 suicide vector pCVD442, and conjugated into *V. cholerae*. Conjugation was performed
583 by mixing and pelleting equal volumes of recipient *V. cholerae* and SM10 or MFD λ*pir*
584 donor LB overnight cultures, spotting the mixed pellet onto LB (+600 μM diaminopimelic
585 acid [DAP] for MFD λ*pir*) followed by incubation at 37°C for 3 hrs. The first round of
586 selection was performed on LB + streptomycin (200 μg $ml^{-1}$ ) + ampicillin (100 μg $ml^{-1}$) at
587 30°C followed by counterselection on salt-free LB + 10% sucrose + streptomycin at room
588 temperature. Inducers for conditionally essential genes were included in all media during
589 conjugation and selection. Addition of 0.2% glucose was required for maintenance in *E.*
590 *coli* of plasmids expressing *Vc mltB*. Deletions were verified by PCR.
591
592 Introduction of a premature stop codon to *mltG* at its native locus to yield Δ7 LTG as well
593 as in-frame deletions of *opgH* were constructed using the pTOX5 *cmR/msqR* allelic
594 exchange system[37]. Flanking regions were cloned into pTOX5 as described for
595 pCVD442. Conjugation was performed by mixing and pelleting equal parts of recipient
596 *V. cholerae* and donor MFD λ*pir*, and spotting onto LB + 1% glucose + 600μM DAP at
597 37°C for 5 hrs. The first round of selection was performed on LB + chloramphenicol (5 μg
598 μg $ml^{-1}$ ) + streptomycin + 1% glucose at 30°C. Chloramphenicol resistant colonies were

599 picked into a 96well plate containing 200μL LB + 1% glucose and incubated at 37°C
600 without agitation for 3 hrs, then counter selected on LB + 1% rhamnose at 30°C.
601 Mutations were verified by PCR.
602
603 Ectopic chromosomal expression from IPTG-inducible $P_{tac}$ was achieved through use of
604 suicide vector pTD101, a pJL1[69] derivative carrying the $P_{tac}$ promoter, a multiple cloning
605 site, and *lacIq* and integrates into the native *V. cholerae lacZ* (*vc2338*) locus. Single
606 genes of interest were amplified from N16961 genomic DNA, introducing a strong
607 consensus RBS (AGGAGA). Genes downstream of *mltG* (*vc2016, vc2015, vc2014*) were
608 amplified together maintaining their native organization, including 30bp upstream of
609 *vc2016* to retain the native RBS. Selection for double crossover events was performed
610 as described for pCVD442. Due to hypersensitivity of the Δ7 LTG strain to β-lactams,
611 ampicillin was reduced to 25 μg $ml^{-1}$ for the first selection. Due to the osmosensitivity of
612 the Δ7 LTG strain, pTD101 in this strain (and control strains) was maintained as an ampR
613 single crossover without counterselection.
614
615 Suicide vector pAM299[70] was used to place *rlpA* under $P_{ara}$ control at its native locus for
616 RlpA depletion experiments. pAM299 was introduced via conjugation and selection for
617 single crossover events on LB + kanamycin (50 μg $ml^{-1}$ ) + streptomycin. IPTG-inducible
618 overexpression of *rlpA-mCherry* fusions for localization studies and *sacB* for levan toxicity
619 assays was achieved using pHL100[70] or its conjugatable derivative pHL100mob. The
620 *sacB* gene was amplified from pCVD442.
621

622 ***Gene insertion/disruption assay for gene essentiality***

623 The suicide vector pAM224 was used to disrupt genes through single crossover
624 integration events. 300bp internal regions in the first third of each respective *orf* (towards
625 the 5' end) were cloned into pAM224 using methods described above. Quantitative
626 conjugation was performed by washing, mixing, and pelleting 500 µL of recipient *V.*
627 *cholerae* and donor MFD λ*pir*. Pellets were re-suspended in 50 µl of LB, spotted onto a
628 45 µm filter on LB + 600 µM DAP, and incubated at 37°C for 4 hrs. Cells were recovered
629 from the filters into 1 ml of LB by vigorous vortexing and 20 µl of the suspension was
630 reserved for 10-fold serial dilution and spotting onto LB + streptomycin (200 µg $ml^{-1}$ )
631 incubated at 30°C to calculate total CFU/ml for all viable *V. cholerae.* The remaining
632 suspension was pelleted and plated on LB + kanamycin (50 µg $ml^{-1}$ ) + streptomycin
633 incubated at 30°C. Viable CFU/ml were calculated, and kanamycin resistance was
634 verified by patching 50 colonies back onto LB + streptomycin +/- kanamycin (all kanR
635 colonies were patched if fewer than 50 colonies were recovered). Transformation
636 efficiency was calculated as a ratio of kanR CFU to all strepR CFU.

637

638 ***Growth rate experiments***

639 Saturated overnight cultures used for growth curve experiments were washed once and
640 resuspended in final growth media, normalizing to $OD_{600}$ 2.0. Normalized cell
641 suspensions were serially diluted into 200 µL growth media and incubated in a Bioscreen
642 growth plate reader (Growth Curves America) at 37°C with random shaking at maximum
643 amplitude, and $OD_{600}$ recorded at 5-min intervals. Calculations of doublings per hour
644 (DPH) were performed in R as previously described[53]. Briefly, logarithmic regressions

645 were fitted to sections of growth curves with >5 consecutive values corresponding to
646 $OD_{600}$ 0.03-0.1 (for $10^{-2}$ diluted inocula) or $OD_{600}$ 0.01-0.1 (for $<10^{-3}$ diluted inocula).
647 Logarithmic regressions of ≥3 replicates with fit value $r^2 > 0.95$ were used to estimate
648 mean doublings per hour for each strain in each growth condition. Growth rates were not
649 calculated for samples that did not reach $OD_{600}$ 0.1, either through absence of detectable
650 growth or lysis prior to reaching $OD_{600}$ 0.1. Growth rates were also not calculated for
651 replicates that were subsequently determined to be suppressors or grew due to
652 irreproducible adaptation. Means within strains between dilution factors and between
653 strains within dilution factors were compared using a two-way Anova and Tukey HSD
654 post-hoc test.
655
656 ***Morphology analysis by microscopy***
657 Strains were grown as described in the figure legends and imaged without fixation on LB
658 0.8% agarose using a Leica DMi8 inverted microscope. Phase-contrast images were
659 analyzed using MicrobeJ. Default parameter settings were applied, and features (septa)
660 were defined as 25% constriction of cell width. Cell outlines were manually edited as
661 needed.
662
663 ***Sacculus composition analysis***
664 PG composition from insoluble sacculi samples were analyzed as described previously
665 with some modifications[71,72]. Briefly, cells were harvested and resuspended and in boiled
666 5% SDS for 1 h. Sacculi were repeatedly washed by ultracentrifugation (110,000 rpm,
667 10 min, 20ºC) with MilliQ water until SDS was totally removed. Samples were treated with

668 20 µg Proteinase K (1 h, 37 °C) for removal of Braun's lipoprotein, and finally treated with
669 muramidase (100 µg/mL) for 16 hours at 37 ºC. Muramidase digestion was stopped by
670 boiling and coagulated proteins were removed by centrifugation (14,000 rpm, 15 min).
671 For sample reduction, the pH of the supernatants was adjusted to pH 8.5-9.0 with sodium
672 borate buffer and sodium borohydride was added to a final concentration of 10 mg/mL.
673 After incubating for 30 min at room temperature, the samples pH was adjusted to pH 3.5
674 with orthophosphoric acid.
675
676 UPLC analyses of muropeptides were performed on a Waters UPLC system (Waters
677 Corporation, USA) equipped with an ACQUITY UPLC BEH C18 Column, 130Å, 1.7 µm,
678 2.1 mm X 150 mm (Waters, USA) and a dual wavelength absorbance detector. Elution of
679 muropeptides was detected at 204 nm. Muropeptides were separated at 45°C using a
680 linear gradient from buffer A (formic acid 0.1% in water) to buffer B (formic acid 0.1% in
681 acetonitrile) in an 18-minute run, with a 0.25 ml/min flow.
682
683 Relative total PG amount was calculated by comparison of the total intensities of the
684 chromatograms (total area) from three biological replicas normalized to the same OD600
685 and extracted with the same volumes. Muropeptide identity was confirmed by MS/MS
686 analysis, using a Xevo G2-XS QTof system (Waters Corporation, USA) (*see next section*
687 *for details*). Quantification of muropeptides was based on their relative abundances
688 (relative area of the corresponding peak) normalized to their molar ratio. Analyses were
689 performed in biological triplicates and means were compared with unpaired t-tests.
690

691 ***Soluble peptidoglycan analysis***

692 Sample preparation of soluble PG samples was performed as follows. Bacteria cultures
693 were harvested by centrifugation (4,000 rpm, 20 min, 4°C). Cell pellets were gently
694 resuspended and washed twice with ice-cold 0.9% NaCl solution. After pelleting the cells
695 again by centrifugation, they were resuspended in 1 ml water and boiled for 30 min.
696 Samples were centrifuged again to remove cell debris at 14,000 rpm for 15 min, and
697 soluble fractions were transferred to new tubes. Next, samples were filtered using 0.2 µm
698 pore size filters. Half of the sample was treated with muramidase (100 µg/mL) for 16 hours
699 at 37 ºC. Muramidase digestion was stopped by boiling and coagulated proteins were
700 removed by centrifugation (14,000 rpm, 15 min). Finally, sample pH was adjusted to pH
701 3.5 with orthophosphoric acid. When needed, samples were diluted or concentrated by
702 speed vacuum.

703

704 Soluble muropeptides were detected and characterized by MS/MS analysis, using a Xevo
705 G2-XS QTof system (Waters Corporation, USA) equipped with an ACQUITY UPLC BEH
706 C18 Column (130 Å, 1.7 µm, 2.1 mm x 150 mm (Waters, USA)). Muropeptides were
707 separated at 45 ºC using a linear gradient from buffer A (formic acid 0.1% in water) to
708 buffer B (formic acid 0.1% in acetonitrile) in an 18-min run, with a 0.25 ml/min flow. The
709 QTOF–MS instrument was operated in positive ionization mode. Detection of
710 muropeptides was performed by $MS^E$ to allow for the acquisition of precursor and product
711 ion data simultaneously, using the following parameters: capillary voltage at 3.0 kV,
712 source temperature to 120 ºC, desolvation temperature to 350 ºC, sample cone voltage
713 to 40 V, cone gas flow 100 l/h, desolvation gas flow 500 l/h and collision energy (CE): low

714 CE: 6 eV and high CE ramp: 15-40 eV. Mass spectra were acquired at a speed of 0.25
715 s/scan. The scan was in a range of 100–2000 *m/z*. Data acquisition and processing was
716 performed using UNIFI software package (Waters Corp.).
717
718 An in-house compound library built in UNIFI was used for detection and identification of
719 muropeptides. Subsequent identification and confirmation of each muropeptide was
720 performed by comparison of the retention-times and mass spectrometric data to known
721 samples. Quantification was performed by integrating peak areas from extracted ion
722 chromatograms (EICs) of the corresponding *m/z* value of each muropeptide and
723 normalized to their molar ratio.
724
725 Soluble muropeptide analyses were performed in biological triplicates and means were
726 compared with unpaired t-tests.
727
728 ***Antibiotic sensitivity***
729 For zone of inhibition assays, a lawn of saturated overnight culture was spread on an LB
730 plate and allowed to dry for 15 minutes. Filter disks (6 mm) were dropped with 5μL of
731 antibiotic solutions (Table S4) onto the lawns and incubated at 37°C for 24 hrs before
732 measurements. Means were compared with a one-way ANOVA and Tukey post-hoc test.
733
734 ***Fluorescent D-amino acid PG labeling***
735 Saturated overnight cultures were diluted 1:100 into LB with 100 μM BADA[47] at 37°C for
736 1.5 hrs before addition of antibiotic. Labeled samples were washed one time in LB before

737 imaging on LB 0.8% agarose pads using a Leica DMi8 inverted microscope set for 490
738 nm excitation.
739

740 ## Acknowledgements

741 We would like to acknowledge Dr. Stephen Zinder (Cornell University) for informative
742 comments based on his unique insight into bacterial physiology. We thank Dr. John
743 Helmann (Cornell University) and members of the Dörr lab for helpful comments on the
744 manuscript. Research on autolysins in the Dörr lab is funded by NIH R01 GM130971.
745 Research in the Cava lab is supported by MIMS, the Knut and Alice Wallenberg
746 Foundation (KAW), the Swedish Research Council and the Kempe Foundation. Research
747 in the VanNieuwenhze lab is supported by the NIH through R01 GM113172 and R35
748 GM136365.
749

750 ## References

751 1 Osawa, M. & Erickson, H. P. Turgor Pressure and Possible Constriction Mechanisms in
752 Bacterial Division. *Frontiers in Microbiology* **9**, doi:10.3389/fmicb.2018.00111 (2018).
753 2 Cabeen, M. T. & Jacobs-Wagner, C. Bacterial cell shape. *Nature Reviews Microbiology* **3**,
754 601-610, doi:10.1038/nrmicro1205 (2005).
755 3 Egan, A. J. F., Errington, J. & Vollmer, W. Regulation of peptidoglycan synthesis and
756 remodelling. *Nature Reviews Microbiology* **18**, 446-460, doi:10.1038/s41579-020-0366-3
757 (2020).
758 4 Zhao, H., Patel, V., Helmann, J. D. & Dörr, T. Don't let sleeping dogmas lie: new views of
759 peptidoglycan synthesis and its regulation. *Mol Microbiol* **106**, 847-860,
760 doi:10.1111/mmi.13853 (2017).
761 5 Sochacki, K. A., Shkel, I. A., Record, M. T. & Weisshaar, J. C. Protein diffusion in the
762 periplasm of E. coli under osmotic stress. *Biophys J* **100**, 22-31,
763 doi:10.1016/j.bpj.2010.11.044 (2011).
764 6 Cho, H. *et al.* Bacterial cell wall biogenesis is mediated by SEDS and PBP polymerase
765 families functioning semi-autonomously. *Nat Microbiol* **1**, 16172,
766 doi:10.1038/nmicrobiol.2016.172 (2016).

767 7 Leclercq, S. *et al.* Interplay between Penicillin-binding proteins and SEDS proteins
768 promotes bacterial cell wall synthesis. *Scientific Reports* **7**, 43306, doi:10.1038/srep43306
769 (2017).
770 8 Taguchi, A. *et al.* FtsW is a peptidoglycan polymerase that is functional only in complex
771 with its cognate penicillin-binding protein. *Nat Microbiol* **4**, 587-594, doi:10.1038/s41564-
772 018-0345-x (2019).
773 9 Nambu, T., Minamino, T., Macnab, R. M. & Kutsukake, K. Peptidoglycan-Hydrolyzing
774 Activity of the FlgJ Protein, Essential for Flagellar Rod Formation inSalmonella
775 typhimurium. *Journal of Bacteriology* **181**, 1555-1561,
776 doi:doi:10.1128/JB.181.5.1555-1561.1999 (1999).
777 10 Santin, Y. G. & Cascales, E. Domestication of a housekeeping transglycosylase for
778 assembly of a Type VI secretion system. *EMBO Rep* **18**, 138-149,
779 doi:10.15252/embr.201643206 (2017).
780 11 Höltje, J. V. Growth of the stress-bearing and shape-maintaining murein sacculus of
781 Escherichia coli. *Microbiol Mol Biol Rev* **62**, 181-203, doi:10.1128/mmbr.62.1.181-
782 203.1998 (1998).
783 12 Herlihey, F. A. & Clarke, A. J. in *Protein Reviews: Volume 17* (ed M. Zouhair Atassi) 41-56
784 (Springer Singapore, 2017).
785 13 Viollier, P. H. & Shapiro, L. A lytic transglycosylase homologue, PleA, is required for the
786 assembly of pili and the flagellum at the Caulobacter crescentus cell pole. *Mol Microbiol*
787 **49**, 331-345, doi:10.1046/j.1365-2958.2003.03576.x (2003).
788 14 Uehara, T. & Park, J. T. Growth of Escherichia coli: significance of peptidoglycan
789 degradation during elongation and septation. *J Bacteriol* **190**, 3914-3922,
790 doi:10.1128/jb.00207-08 (2008).
791 15 Nguyen, L. T., Gumbart, J. C., Beeby, M. & Jensen, G. J. Coarse-grained simulations of
792 bacterial cell wall growth reveal that local coordination alone can be sufficient to maintain
793 rod shape. *Proceedings of the National Academy of Sciences* **112**, E3689-E3698,
794 doi:10.1073/pnas.1504281112 (2015).
795 16 Lee, T. K. & Huang, K. C. The role of hydrolases in bacterial cell-wall growth. *Current*
796 *opinion in microbiology* **16**, 760-766, doi:10.1016/j.mib.2013.08.005 (2013).
797 17 Murphy, S. G. *et al.* Class A Penicillin-Binding Protein-Mediated Cell Wall Synthesis
798 Promotes Structural Integrity during Peptidoglycan Endopeptidase Insufficiency in Vibrio
799 cholerae. *mBio* **12**, doi:10.1128/mBio.03596-20 (2021).
800 18 Singh, S. K., SaiSree, L., Amrutha, R. N. & Reddy, M. Three redundant murein
801 endopeptidases catalyse an essential cleavage step in peptidoglycan synthesis of
802 Escherichia coli K12. *Mol Microbiol* **86**, 1036-1051, doi:10.1111/mmi.12058 (2012).
803 19 Byun, B. *et al.* Mechanism of the Escherichia coli MltE lytic transglycosylase, the cell-wall-
804 penetrating enzyme for Type VI secretion system assembly. *Sci Rep* **8**, 4110,
805 doi:10.1038/s41598-018-22527-y (2018).
806 20 Dik, D. A., Marous, D. R., Fisher, J. F. & Mobashery, S. Lytic transglycosylases: concinnity
807 in concision of the bacterial cell wall. *Crit Rev Biochem Mol Biol* **52**, 503-542,
808 doi:10.1080/10409238.2017.1337705 (2017).

809 21 Lee, M. *et al.* Exolytic and endolytic turnover of peptidoglycan by lytic transglycosylase Slt
810 of Pseudomonas aeruginosa. *Proceedings of the National Academy of*
811 *Sciences* **115**, 4393-4398, doi:10.1073/pnas.1801298115 (2018).
812 22 Vijayaraghavan, J. *et al.* Structural studies and molecular dynamics simulations suggest a
813 processive mechanism of exolytic lytic transglycosylase from Campylobacter jejuni. *PLOS*
814 *ONE* **13**, e0197136, doi:10.1371/journal.pone.0197136 (2018).
815 23 Höltje, J. V., Mirelman, D., Sharon, N. & Schwarz, U. Novel type of murein transglycosylase
816 in Escherichia coli. *J Bacteriol* **124**, 1067-1076, doi:10.1128/jb.124.3.1067-1076.1975
817 (1975).
818 24 Williams, A. H. *et al.* A step-by-step in crystallo guide to bond cleavage and 1,6-anhydro-
819 sugar product synthesis by a peptidoglycan-degrading lytic transglycosylase. *J Biol Chem*
820 **293**, 6000-6010, doi:10.1074/jbc.RA117.001095 (2018).
821 25 Kraft, A. R., Templin, M. F. & Höltje, J. V. Membrane-bound lytic endotransglycosylase in
822 Escherichia coli. *Journal of bacteriology* **180**, 3441-3447, doi:10.1128/JB.180.13.3441-
823 3447.1998 (1998).
824 26 Bohrhunter, J. L., Rohs, P. D. A., Torres, G., Yunck, R. & Bernhardt, T. G. MltG activity
825 antagonizes cell wall synthesis by both types of peptidoglycan polymerases in Escherichia
826 coli. *Molecular Microbiology* **115**, 1170-1180, doi:https://doi.org/10.1111/mmi.14660
827 (2021).
828 27 Yunck, R., Cho, H. & Bernhardt, T. G. Identification of MltG as a potential terminase for
829 peptidoglycan polymerization in bacteria. *Molecular Microbiology* **99**, 700-718,
830 doi:10.1111/mmi.13258 (2016).
831 28 Sassine, J., Pazos, M., Breukink, E. & Vollmer, W. Lytic transglycosylase MltG cleaves in
832 nascent peptidoglycan and produces short glycan strands. *The Cell Surface* **7**, 100053,
833 doi:https://doi.org/10.1016/j.tcsw.2021.100053 (2021).
834 29 Tsui, H. C. *et al.* Suppression of a deletion mutation in the gene encoding essential PBP2b
835 reveals a new lytic transglycosylase involved in peripheral peptidoglycan synthesis in
836 Streptococcus pneumoniae D39. *Mol Microbiol* **100**, 1039-1065, doi:10.1111/mmi.13366
837 (2016).
838 30 Koraimann, G. Lytic transglycosylases in macromolecular transport systems of Gram-
839 negative bacteria. *Cell Mol Life Sci* **60**, 2371-2388, doi:10.1007/s00018-003-3056-1
840 (2003).
841 31 Jacobs, C., Huang, L. J., Bartowsky, E., Normark, S. & Park, J. T. Bacterial cell wall recycling
842 provides cytosolic muropeptides as effectors for beta-lactamase induction. *Embo j* **13**,
843 4684-4694 (1994).
844 32 Dik, D. A., Fisher, J. F. & Mobashery, S. Cell-Wall Recycling of the Gram-Negative Bacteria
845 and the Nexus to Antibiotic Resistance. *Chem Rev* **118**, 5952-5984,
846 doi:10.1021/acs.chemrev.8b00277 (2018).
847 33 Heidrich, C., Ursinus, A., Berger, J., Schwarz, H. & Holtje, J. V. Effects of multiple deletions
848 of murein hydrolases on viability, septum cleavage, and sensitivity to large toxic
849 molecules in Escherichia coli. *J Bacteriol* **184**, 6093-6099, doi:10.1128/jb.184.22.6093-
850 6099.2002 (2002).
851 34 Jorgenson, M. A., Chen, Y., Yahashiri, A., Popham, D. L. & Weiss, D. S. The bacterial septal
852 ring protein RlpA is a lytic transglycosylase that contributes to rod shape and daughter

853 cell separation in Pseudomonas aeruginosa. *Mol Microbiol* **93**, 113-128,
854 doi:10.1111/mmi.12643 (2014).
855 35 Weaver, A. I. *et al.* Lytic transglycosylases RlpA and MltC assist in Vibrio cholerae daughter
856 cell separation. *Molecular Microbiology* **112**, 1100-1115, doi:10.1111/mmi.14349 (2019).
857 36 Priyadarshini, R., Popham, D. L. & Young, K. D. Daughter cell separation by penicillin-
858 binding proteins and peptidoglycan amidases in Escherichia coli. *Journal of bacteriology*
859 **188**, 5345-5355, doi:10.1128/JB.00476-06 (2006).
860 37 Lazarus, J. E. *et al.* A New Suite of Allelic-Exchange Vectors for the Scarless Modification
861 of Proteobacterial Genomes. *Appl Environ Microbiol* **85**, doi:10.1128/aem.00990-19
862 (2019).
863 38 Deutscher, J. *et al.* The bacterial phosphoenolpyruvate:carbohydrate phosphotransferase
864 system: regulation by protein phosphorylation and phosphorylation-dependent protein-
865 protein interactions. *Microbiol Mol Biol Rev* **78**, 231-256, doi:10.1128/mmbr.00001-14
866 (2014).
867 39 Bontemps-Gallo, S., Bohin, J. & Lacroix, J. Osmoregulated Periplasmic Glucans. *EcoSal*
868 *Plus*, doi:doi:10.1128/ecosalplus.ESP-0001-2017 (2017).
869 40 Hill, N. S., Buske, P. J., Shi, Y. & Levin, P. A. A Moonlighting Enzyme Links Escherichia coli
870 Cell Size with Central Metabolism. *PLOS Genetics* **9**, e1003663,
871 doi:10.1371/journal.pgen.1003663 (2013).
872 41 Quintard, K. *et al.* Evaluation of the Role of the opgGH Operon in Yersinia
873 pseudotuberculosis and Its Deletion during the Emergence of Yersinia pestis. *Infection*
874 *and immunity* **83**, 3638-3647, doi:10.1128/IAI.00482-15 (2015).
875 42 Tanaka, T., Oi, S. & Yamamoto, T. The molecular structure of low and high molecular
876 weight levans synthesized by levansucrase. *J Biochem* **87**, 297-303,
877 doi:10.1093/oxfordjournals.jbchem.a132737 (1980).
878 43 Steinmetz, M., Le Coq, D., Djemia, H. B. & Gay, P. [Genetic analysis of sacB, the structural
879 gene of a secreted enzyme, levansucrase of Bacillus subtilis Marburg]. *Mol Gen Genet* **191**,
880 138-144, doi:10.1007/bf00330901 (1983).
881 44 Gay, P., Le Coq, D., Steinmetz, M., Ferrari, E. & Hoch, J. A. Cloning structural gene sacB,
882 which codes for exoenzyme levansucrase of Bacillus subtilis: expression of the gene in
883 Escherichia coli. *J Bacteriol* **153**, 1424-1431, doi:10.1128/jb.153.3.1424-1431.1983
884 (1983).
885 45 Blomfield, I. C., Vaughn, V., Rest, R. F. & Eisenstein, B. I. Allelic exchange in Escherichia coli
886 using the Bacillus subtilis sacB gene and a temperature-sensitive pSC101 replicon.
887 *Molecular Microbiology* **5**, 1447-1457, doi:https://doi.org/10.1111/j.1365-
888 2958.1991.tb00791.x (1991).
889 46 Cho, H., Uehara, T. & Bernhardt, T. G. Beta-lactam antibiotics induce a lethal
890 malfunctioning of the bacterial cell wall synthesis machinery. *Cell* **159**, 1300-1311,
891 doi:10.1016/j.cell.2014.11.017 (2014).
892 47 Hsu, Y. P. *et al.* Full color palette of fluorescent d-amino acids for in situ labeling of
893 bacterial cell walls. *Chem Sci* **8**, 6313-6321, doi:10.1039/c7sc01800b (2017).
894 48 Kuru, E. *et al.* In Situ probing of newly synthesized peptidoglycan in live bacteria with
895 fluorescent D-amino acids. *Angew Chem Int Ed Engl* **51**, 12519-12523,
896 doi:10.1002/anie.201206749 (2012).

897 49 Barreteau, H. *et al.* Cytoplasmic steps of peptidoglycan biosynthesis. *FEMS Microbiology*
898 *Reviews* **32**, 168-207, doi:10.1111/j.1574-6976.2008.00104.x (2008).
899 50 Dorr, T., Cava, F., Lam, H., Davis, B. M. & Waldor, M. K. Substrate specificity of an
900 elongation-specific peptidoglycan endopeptidase and its implications for cell wall
901 architecture and growth of Vibrio cholerae. *Mol Microbiol* **89**, 949-962,
902 doi:10.1111/mmi.12323 (2013).
903 51 Chaput, C., Labigne, A. & Boneca, I. G. Characterization of Helicobacter pylori lytic
904 transglycosylases Slt and MltD. *J Bacteriol* **189**, 422-429, doi:10.1128/jb.01270-06 (2007).
905 52 Scheurwater, E. M. & Clarke, A. J. The C-terminal Domain of Escherichia coli YfhD
906 Functions as a Lytic Transglycosylase*. *Journal of Biological Chemistry* **283**, 8363-8373,
907 doi:https://doi.org/10.1074/jbc.M710135200 (2008).
908 53 Mueller, E. A., Egan, A. J. F., Breukink, E., Vollmer, W. & Levin, P. A. Plasticity of Escherichia
909 coli cell wall metabolism promotes fitness and antibiotic resistance across environmental
910 conditions. *eLife* **8**, e40754, doi:10.7554/eLife.40754 (2019).
911 54 Yakhnina, A. A. & Bernhardt, T. G. The Tol-Pal system is required for peptidoglycan-
912 cleaving enzymes to complete bacterial cell division. *Proceedings of the National Academy*
913 *of Sciences* **117**, 6777-6783, doi:10.1073/pnas.1919267117 (2020).
914 55 Suzuki, M., Hara, H. & Matsumoto, K. Envelope disorder of Escherichia coli cells lacking
915 phosphatidylglycerol. *J Bacteriol* **184**, 5418-5425, doi:10.1128/jb.184.19.5418-5425.2002
916 (2002).
917 56 Romeis, T. & Holtje, J. V. Specific interaction of penicillin-binding proteins 3 and 7/8 with
918 soluble lytic transglycosylase in Escherichia coli. *J Biol Chem* **269**, 21603-21607 (1994).
919 57 Vollmer, W., von Rechenberg, M. & Holtje, J. V. Demonstration of molecular interactions
920 between the murein polymerase PBP1B, the lytic transglycosylase MltA, and the
921 scaffolding protein MipA of Escherichia coli. *J Biol Chem* **274**, 6726-6734,
922 doi:10.1074/jbc.274.10.6726 (1999).
923 58 Legaree, B. A. & Clarke, A. J. Interaction of penicillin-binding protein 2 with soluble lytic
924 transglycosylase B1 in Pseudomonas aeruginosa. *J Bacteriol* **190**, 6922-6926,
925 doi:10.1128/JB.00934-08 (2008).
926 59 Cooper, S., Hsieh, M. L. & Guenther, B. Mode of peptidoglycan synthesis in Salmonella
927 typhimurium: single-strand insertion. *J Bacteriol* **170**, 3509-3512,
928 doi:10.1128/jb.170.8.3509-3512.1988 (1988).
929 60 de Jonge, B. L. *et al.* Peptidoglycan synthesis during the cell cycle of Escherichia coli:
930 composition and mode of insertion. *J Bacteriol* **171**, 5783-5794,
931 doi:10.1128/jb.171.11.5783-5794.1989 (1989).
932 61 Burman, L. G. & Park, J. T. Molecular model for elongation of the murein sacculus of
933 Escherichia coli. *Proc Natl Acad Sci U S A* **81**, 1844-1848, doi:10.1073/pnas.81.6.1844
934 (1984).
935 62 Koch, A. L. The three-for-one model for Gram-negative wall growth: a problem and a
936 possible solution. *FEMS Microbiology Letters* **162**, 127-134, doi:10.1111/j.1574-
937 6968.1998.tb12989.x (1998).
938 63 Meisner, J. *et al.* FtsEX is required for CwlO peptidoglycan hydrolase activity during cell
939 wall elongation in Bacillus subtilis. *Mol Microbiol* **89**, 1069-1083, doi:10.1111/mmi.12330
940 (2013).

941 64 Voedts, H. *et al.* Role of endopeptidases in peptidoglycan synthesis mediated by
942 alternative cross-linking enzymes in Escherichia coli. *bioRxiv*,
943 2021.2002.2012.430937, doi:10.1101/2021.02.12.430937 (2021).
944 65 Heidelberg, J. F. *et al.* DNA sequence of both chromosomes of the cholera pathogen Vibrio
945 cholerae. *Nature* **406**, 477-483, doi:10.1038/35020000 (2000).
946 66 Ferrières, L. *et al.* Silent mischief: bacteriophage Mu insertions contaminate products of
947 Escherichia coli random mutagenesis performed using suicidal transposon delivery
948 plasmids mobilized by broad-host-range RP4 conjugative machinery. *J Bacteriol* **192**,
949 6418-6427, doi:10.1128/jb.00621-10 (2010).
950 67 Gibson, D. G. *et al.* Enzymatic assembly of DNA molecules up to several hundred kilobases.
951 *Nat Methods* **6**, 343-345, doi:10.1038/nmeth.1318 (2009).
952 68 Donnenberg, M. S. & Kaper, J. B. Construction of an eae deletion mutant of
953 enteropathogenic Escherichia coli by using a positive-selection suicide vector. *Infection*
954 *and immunity* **59**, 4310-4317, doi:10.1128/iai.59.12.4310-4317.1991 (1991).
955 69 Miyata, S. T., Unterweger, D., Rudko, S. P. & Pukatzki, S. Dual expression profile of type VI
956 secretion system immunity genes protects pandemic Vibrio cholerae. *PLoS pathogens* **9**,
957 e1003752-e1003752, doi:10.1371/journal.ppat.1003752 (2013).
958 70 Möll, A. *et al.* A D, D-carboxypeptidase is required for Vibrio cholerae halotolerance.
959 *Environ Microbiol* **17**, 527-540, doi:10.1111/1462-2920.12779 (2015).
960 71 Alvarez, L., Hernandez, S. B., de Pedro, M. A. & Cava, F. in *Bacterial Cell Wall Homeostasis:*
961 *Methods and Protocols* (ed Hee-Jeon Hong) 11-27 (Springer New York, 2016).
962 72 Desmarais, S. M., De Pedro, M. A., Cava, F. & Huang, K. C. Peptidoglycan at its peaks: how
963 chromatographic analyses can reveal bacterial cell wall structure and assembly. *Mol*
964 *Microbiol* **89**, 1-13, doi:10.1111/mmi.12266 (2013).
965